Analytica Chimica Acta 1058 (2019) 29–38

Contents lists available at ScienceDirect

Analytica Chimica Acta

journal homepage: www.elsevier.com/locate/aca

Quantitative analysis of asbestos in drinking water and its migration in mice using fourier-transform infrared spectroscopy and inductively coupled plasma optical emission spectrometry

Bei Zheng [a], Lijie Zang [a], Wentao Li [b], Hongyan Li [a, *], Haitao Wang [c], Ming Zhang [d], Xiaohong Song [e]

[a] Key Laboratory of Drinking Water Science and Technology, Chinese Academy of Sciences, Beijing, 100085, China
[b] Shenzhen Institute of Information Technology, Shenzhen, 518172, China
[c] First Affiliated Hospital of PLA General Hospital, Beijing, 100048, China
[d] Zhejiang University of Technology, College of Environment, Hangzhou, 310034, China
[e] Shimadzu (China) Co., Ltd., Beijing, 100020, China

HIGHLIGHTS

- A technique using Fourier-transform infrared spectroscopy for quantitatively analyzing asbestos was developed.
- Asbestos was quantified (silicon dioxide present) using differential spectrum and partial least squares methods.
- Migration of ingested asbestos in mouse organs and blood was investigated.
- Asbestos fibers in water could pose unpredictable risks to humans.

GRAPHICAL ABSTRACT

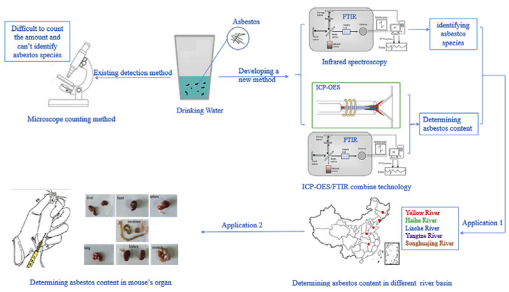

ARTICLE INFO

Article history:
Received 14 May 2018
Received in revised form
13 December 2018
Accepted 15 December 2018
Available online 19 December 2018

Keywords:
Asbestos
Quantitative analysis
FT-IR
ICP-OES
Drinking water
Asbestos migration

ABSTRACT

The presence of asbestos in the environment has caused concern because exposure to asbestos can cause diseases such as stomach and pancreatic cancer. However, suitable up-to-date methods for quantitatively analyzing asbestos and assessing the toxicity of asbestos have not been developed. In this study, asbestos in drinking water was characterized using a stepwise multiple differential infra-red spectra method and a partial least squares method. The in vivo migration of ingested asbestos in mice was then investigated using the technique. The quantification limit of six kinds of asbestos by using inductively coupled plasma optical emission spectrometry and Fourier-transform infrared spectroscopy in water are respectively from 0.0468 to 0.0705 mg/L, from 0.0039 to 0.0064 mg/L. The relative standard deviations were respectively less than 2.85% and 3.81%. The recoveries of the test asbestos were respectively more than 95.10% and 95.38%. Asbestos was found mainly to accumulate in the livers of mice. The Fourier-transform infra-red spectroscopy inductively coupled plasma optical emission spectrometry method can be used to detect and precisely quantify asbestos in water samples and in animal tissues.

* Corresponding author.
E-mail address: hyli@rcees.ac.cn (H. Li).

https://doi.org/10.1016/j.aca.2018.12.022
0003-2670/

1. Introduction

Asbestos is a group of nonspecific fibrous silicate minerals containing hydrogen, calcium, iron, magnesium, oxygen, silicon, and sodium. Asbestos is classed as a class A carcinogen by the International Organization for Cancer Research and a priority pollutant by the US Environmental Protection Agency [1,2]. Inhaled asbestos has been found to cause lung diseases including asbestosis, lung tumors, and malignant mesothelioma. No evidence has been found for ingested asbestos causing cancer, but the public has nevertheless been concerned about exposure to asbestos entering water from minerals, industrial waste, or deteriorating asbestos–cement pipes in water distribution systems [3]. Asbestos fibers have been found to be toxic because of the synergistic effects of the fiber sizes, fiber types, crystal structures, and surface reactivities [4–9]. The toxicity of asbestos to humans has been underestimated because of the limitations of methods previously used to detect asbestos. Few studies have been focused on the migration of asbestos in animals in vivo although it is very important to explore the mechanism(s) through which ingested asbestos may cause cancer. Both fibrosis and epithelial tumors are very dependent on the ability of epithelial cells to be transformed into mesenchymal cells through the epithelial–mesenchymal transition process [10,11]. It is important to gain an understanding of this process after the ingestion of asbestos. Currently available gravimetric and microscopic examination methods are not suitable for studying the migration of asbestos in vivo.

The counting method, which requires a series of pretreatments, has been widely used to quantify asbestos fibers in environmental samples [12], but it is difficult to rapidly and accurately determine the asbestos content using a limited microscope field [13], especially for asbestos in animal tissues. The gravimetric method is often used to quantify asbestos in environmental samples, but this simple and convenient method cannot distinguish the types of asbestos fibers. Between Fourier-transform infrared spectroscopy (FT-IR) has been used to identify different types of asbestos [14,15]. Silicon is considered to be an indicative element for asbestos. Coupling FT-IR with inductively coupled plasma optical emission spectrometry (ICP-OES) to allow silicon to be quantified could be a novel way of measuring asbestos in water and animal tissues. This technique would also avoid interferences from silicates when quantitatively analyzing asbestos.

The aim of this work was to qualitatively and quantitatively analyze asbestos in water and to trace the migration of asbestos in animals in vivo. Achieving these aims would improve our understanding of the harm caused by asbestos ingested in drinking water. The FT-IR technique combined with data processing methods (stepwise multiple differential FT-IR spectrum processing and the partial least squares method) was developed and used to identify different asbestos species. Six types of asbestos found widely in the environment were selected as targets. Asbestos was mixed with kaolin and sand to simulate complex environmental water samples. Asbestos ingested by mice was analyzed to study the migration of asbestos through the organs. The data were expected to provide insights into the risks to human health posed by asbestos released from deteriorating asbestos–cement pipes in water distribution systems.

2. Materials and methods

2.1. Chemicals

Six kinds of asbestos (actinolite, amosite, anthophyllite, chrysotile, crocidolite, and tremolite asbestos) were provided by the Health & Safety Laboratory (Buxton, UK). The chemical compositions and appearances of the asbestos samples are shown in Table S1 and Fig. S1 in the Supporting Information (SI). Asbestos is composed of Al, Ca, Fe, Mg, Na, and Si and typically has fibrous clusters. All containers used in the analyses were made of polytetrafluoroethylene to avoid the samples becoming contaminated with Si.

Mixed cellulose ester membranes (bore diameter 0.2 μm) and silver filters were purchased from Merck Co. (Kenilworth, NJ, USA) and Sterlitech Co. (Kent, Maryland, USA), respectively. A fiber slicer and ball mill were obtained from Beijing Tech-Service Technology Co. (Beijing, China). Balb/c mice were provided by Beijing Vital River Laboratory Animal Technology Co. (Beijing, China).

2.2. Quantitative analysis of asbestos in aqueous samples under various conditions

2.2.1. Water sample pretreatment

Each sample was enriched by passing it through a mixed cellulose membrane, then the membrane was washed with HCl and then ultrapure water to remove impurities. The membrane was then dissolved in acetone and the mixture was passed through a pure silver membrane. The silver membrane was then placed in a muffle furnace at 220 °C for 30 min to remove organic matter.

Before ICP-OES analysis, each enriched sample was mixed with 0.5 g KOH or NaOH in a platinum crucible, then the mixture was melted at 600 °C in a muffle furnace and shaken twice during the heating process. Once the sample was completely melted it was removed from the furnace and cooled, then a small amount of ultrapure water was added, and the solution was transferred to a beaker. The platinum crucible was rinsed with HCl twice, and the rinses were mixed with the solution in the beaker. The solution was adjusted to pH 7 ± 0.5 (using HCl/NaOH to adjust the pH of the solution by pH meter) and diluted to 100 mL in a volumetric flask. The concentrations of the elements of interest in the solution were determined by ICP-OES.

2.2.2. Acquisition of asbestos FT-IR spectra

Pretreated asbestos was cut using a fiber slicer, then mixed with potassium bromide in a ball mill, and the mixture was pressed into a spindle piece for FT-IR analysis. A Nicolet 8700 attenuated total reflectance FT-IR spectrometer (Thermo Fisher Waltham, MA, USA) was used to collect spectra over the range 4000–600 cm^{-1} using a scan frequency of 32 s^{-1} and a resolution of 4 cm^{-1}. Each sample was formed into three pieces, and five points on each piece were analyzed by FT-IR.

2.2.3. Detecting asbestos in mixed asbestos–particle systems

Silicon is the second most abundant element in the natural environment, and most silicon in groundwater is present as silica (Fig. S2 in SI). Natural water containing particles was simulated by adding 5 mg SiO_2 and 5 mg asbestos to ultrapure water. Each sample was enriched and purified (see Section 2.2.1), then treated using a fiber slicer and mixed with KBr at a KBr:sample mass ratio of 1:100 in a ball mill. Non-overlapping characteristic peaks in the FT-IR spectrum were used to identify and characterize the asbestos. As shown in Fig. S3 (in SI), peaks at 3650–3670 cm^{-1} were characteristic peaks for asbestos that were not affected by particles present at different mixing ratios.

2.2.4. Partial least squares method for analyzing multiple types of asbestos

Chrysotile and actinolite were mixed at chrysotile:actinolite mass ratios of 0:100, 10:90, 20:80, 30:70, 40:60, 50:50, 60:40, 70:30, 80:20, 90:10, and 100:0, then each mixture was made into a powder and mixed with KBr at a KBr:sample mass ratio of 1:100.

Table 1
The LOD and LOQ of 6 kinds of asbestos by ICP-OES in ultrapure water.

Asbestos species	LOD, mg/L	LOQ, mg/L
Chrysotile	0.0197	0.0665
Crocidolite	0.0173	0.0585
Amosite	0.0209	0.0705
Anthophyllite asbestos	0.0209	0.0705
Tremolite asbestos	0.0139	0.0468
Actinolite asbestos	0.0195	0.0657

Each mixture was ground in an agate mortar, then divided into three equal portions. Each portion was pressed into a flat layer, then five points on each sample were analyzed by FT-IR. The test conditions were the same as described in Section 2.2.2.

2.3. Asbestos migration within mice

The male Balb/c mice weighed between 21 and 25 g. Ten male mice were randomly divided into five groups, and the two mice in each group were given the numbers 1 and 2. All the No. 1 mice were fed 0.5 mL chrysotile suspension (about 1 mg d^{-1}) each day, and all the No. 2 mice were fed 0.5 mL drinking water (in addition to the normal drinking water) each day. After 5 d, the No. 1 mice started to be fed drinking water and nutrient solution instead of the chrysotile suspension each day. On the seventh day, the mice in the first group were dissected and samples of blood, small intestine, liver, and spleen were collected. Each tissue sample was dried at 40 °C for 48 h, then quantitatively analyzed using the FT-IR, ICP-OES respectively method. The mice in groups 2, 3, 4, and 5 were treated in the same way on the 15th, 30th, 45th, and 60th days, respectively.

3. Results and discussion

3.1. Qualitative theory of analyzing asbestos by FT-IR

The quantitative analysis method was based on similarities between the FT-IR spectra of the samples and standard materials, using correlation coefficients, angle cosines, distance coefficients [16,17], and other parameters.

$$r = \frac{\sum (a_i - \overline{a})\left(b_i - \overline{b}\right)}{\sqrt{\sum (a_i - \overline{a})^2 \sum \left(b_i - \overline{b}\right)^2}} \quad (1)$$

In Equation (1), a_i and b_i are the responses in the sample spectrum and standard spectrum, respectively, and $\overline{a}$ and $\overline{b}$ are the mean responses, respectively. The closer the correlation coefficient r was to 1 the more the sample spectrum resembled the standard material spectrum. The method was limited by the precision and stability of the FT-IR spectra, and two spectra were considered to be consistent at a similarity of $\geq$0.999, otherwise they were considered to be different.

The differential spectrum method means a method for obtaining the spectrum of one component in a two-component mixture by subtracting the spectrum of the other component. Asbestos was identified by comparing an obtained spectrum with a standard material spectrum, as described in the previous paragraph. In a multiple-component mixture, multiple differential spectra will be obtained with the aim of identifying the components by subtracting spectra step by step.

Table 2
The LOD and LOQ of 6 kinds of asbestos by FT-IR in water.

Asbestos species	Regression equation	Correlation coefficient (r^2)	LOD, mg/L	LOQ, mg/L
Crocidolite	Y = 1.3166X+0.0255	0.9995	0.0015	0.0051
Chrysotile	Y = 10.561X+0.3329	0.9991	0.0019	0.0064
Amosite	Y = 5.0799X-0.1329	0.9991	0.0012	0.0039
Actinolite asbestos	Y = 1.2343X+0.0474	0.9990	0.0017	0.0055
Tremolite asbestos	Y = 2.2773X+0.0336	0.9998	0.0013	0.0043
Anthophyllite asbestos	Y = 1.2913X+0.0174	0.9998	0.0016	0.0052

Table 3
The RSD and recovery of asbestos spiked in the Songhua River water by ICP-OES (n = 6).

Asbestos	blank	Amout spiked (mg/L)	Mean ± SD (mg/L)	RSD (%)	Recovery (%)
Chrysotile	<0.0197	0.490	0.472 ± 0.0129	2.74	96.39
		2.460	2.471 ± 0.0082	0.33	100.45
		4.930	4.816 ± 0.1241	2.58	97.69
Crocidolite	<0.0173	0.433	0.427 ± 0.0072	1.68	98.69
		2.165	2.168 ± 0.0160	0.74	100.15
		4.330	4.283 ± 0.0322	0.75	98.90
Tremolite asbestos	<0.0139	0.346	0.331 ± 0.0094	2.85	95.42
		1.732	1.752 ± 0.0114	0.65	101.12
		3.464	3.462 ± 0.0046	0.13	99.93
Actinolite asbestos	<0.0195	0.487	0.463 ± 0.0060	1.30	95.10
		2.433	2.344 ± 0.0456	1.94	96.33
		4.866	4.812 ± 0.0589	1.22	98.88
Amosite	<0.0209	0.522	0.500 ± 0.0073	1.47	95.70
		2.612	2.614 ± 0.0063	0.24	100.07
		5.223	5.163 ± 0.0572	1.11	98.85
Anthophyllite asbestos	<0.0209	0.522	0.498 ± 0.0116	2.34	95.32
		2.612	2.678 ± 0.0537	2.01	102.54
		5.223	5.218 ± 0.0089	1.11	99.27

RSD, relative standard deviation.

Table 4
The RSD and recovery of asbestos spiked in the Songhua River water by FT-IR (n = 6).

Asbestos	blank	Amout spiked (mg/L)	Mean ± SD (mg/L)	RSD (%)	Recovery (%)
Chrysotile	<0.0015	0.5	0.507 ± 0.0104	2.06	101.37
		1.0	0.989 ± 0.0077	0.77	98.89
		1.5	1.482 ± 0.0133	0.90	98.80
Crocidolite	<0.0019	0.5	0.481 ± 0.0106	2.21	96.15
		1.0	1.002 ± 0.0201	0.20	100.16
		1.5	1.473 ± 0.0126	0.85	98.20
Tremolite asbestos	<0.0013	0.5	0.477 ± 0.0182	3.81	95.38
		1.0	0.978 ± 0.0193	1.97	97.77
		1.5	1.482 ± 0.0159	1.07	98.78
Actinolite asbestos	<0.0017	0.5	0.498 ± 0.0077	2.02	98.39
		1.0	1.036 ± 0.0025	0.24	103.64
		1.5	1.495 ± 0.0084	0.56	99.68
Amosite	<0.0012	0.5	0.501 ± 0.0057	1.14	100.26
		1.0	0.974 ± 0.0194	1.99	97.44
		1.5	1.476 ± 0.0154	1.04	98.44
Anthophyllite asbestos	<0.0016	0.5	0.502 ± 0.0061	1.22	100.32
		1.0	0.966 ± 0.0021	0.22	96.58
		1.5	1.502 ± 0.0114	0.76	100.13

RSD, relative standard deviation.

3.2. Validation of the assay

3.2.1. Limit of detection (LOD) and limit of quantification (LOQ)

Calibration curves were obtained for asbestos using a series of Si calibration standard solutions. Limit of detection (LOD) is defined as the lowest concentration level that is statistically different from a blank (LOD = 3SD/m; m is the slope of the addition graph, SD is the within-run standard deviation of single blank determination), corresponding to a 99% confidence level. Similarly, limit of quantification (LOQ) is defined as LOQ = 10 SD/m[18]. When determining the LOD and LOQ of asbestos by infrared spectroscopy, blank tests have been carried out in the band corresponding to the quantitative characteristic peak position. The concentration of asbestos in ultrapure water are detected by determining the element Si when using ICP-OES. This examination demonstrated a linear relationship with correlation coefficients being greater than 0.990. Linear equations were Y = 11592X-972.85 for Si element in the concentration range of 0.01–2 mg/L. The LOD and LOQ of the asbestos are calculated by the Si percentage content in the chemical formula. The LOD of six kinds of asbestos by using ICP-OES and FT-IR in water are respectively from 0.0139 to 0.0209 mg/L, from 0.0012 to 0.0019 mg/L as shown in Table 1 and Table 2, and The LOQ of six kinds of asbestos by using ICP-OES and FT-IR in water are respectively from 0.0468 to 0.0705 mg/L, from 0.0039 to 0.0064 mg/L.

3.2.2. Precision and accuracy

Validation of the method developed in this study was performed [18]. Three levels for each type of asbestos were used to estimate recovery, and six replicates at each concentration level of six types of asbestos were evaluated. To calculate the standard deviation values for precision and accuracy, 1 L of Songhua River samples spiked with 0.346 and 5.223 mg/L of six types of asbestos were tested using ICP-OES, while spiked with 0.5 and 1.5 mg/L asbestos were detected when using FT-IR. The relative standard deviation (RSD) results were less than 2.85% and 3.81% using ICP-OES and FT-IR, respectively. And the recoveries were respectively more than 95.10% and 95.38% with ICP-OES and FT-IR, respectively. Results are shown in Table 3 and Table 4.

3.3. Quantitative analysis of asbestos in mixed samples by FT-IR and ICP-OES

Particulate matter in water is mainly clay and organic particulate matter. Clays are natural minerals with aluminosilicate structures that also contain SiO_2, e.g., sand and kaolin [19–22]. Most particulate matter can be removed during drinking-water treatment processes, but some particles remain in tap water. If such particles were removed by the silver filter it would not have been possible to remove them from the sample collected by the silver filter using the enrichment and purification method described above. When developing the method for analyzing asbestos in mixtures of asbestos and SiO_2 sand we paid particular attention to the influence of SiO_2 on the location of the characteristic asbestos peak in the FT-IR spectrum, as shown in Fig. 1. Taking chrysotile as an example, the peak at 3686 cm^{-1} was selected as the characteristic FT-IR peak (Fig. S3 in SI). The peak at 3686 cm^{-1} did not move but the intensity increased as the SiO_2 content decreased (Fig. 1), indicating that SiO_2 sand did not interfere with this characteristic FT-IR peak and that the peak could be used to indicate the presence of chrysotile.

The FT-IR spectra of SiO_2 and asbestos mixtures after the pretreatment method had been performed were acquired using the differential spectrum method. The FT-IR spectral similarities of the mixed samples and standard asbestos materials were calculated by

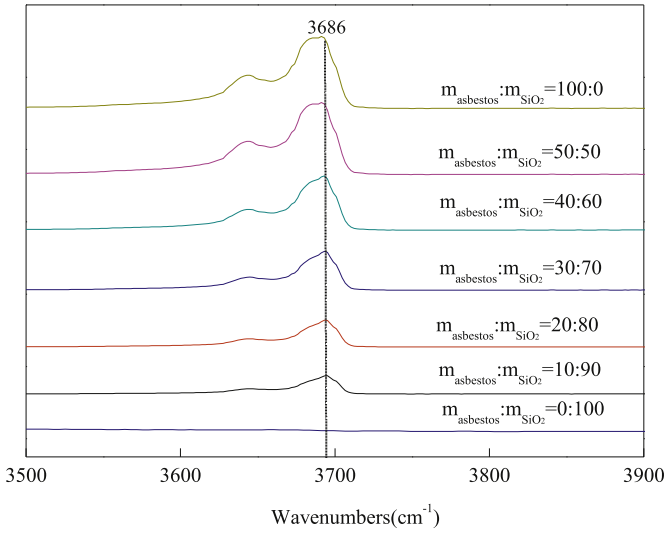

Fig. 1. Characteristic FT-IR peaks of mixtures of chrysotile and SiO_2 at different mass ratios.

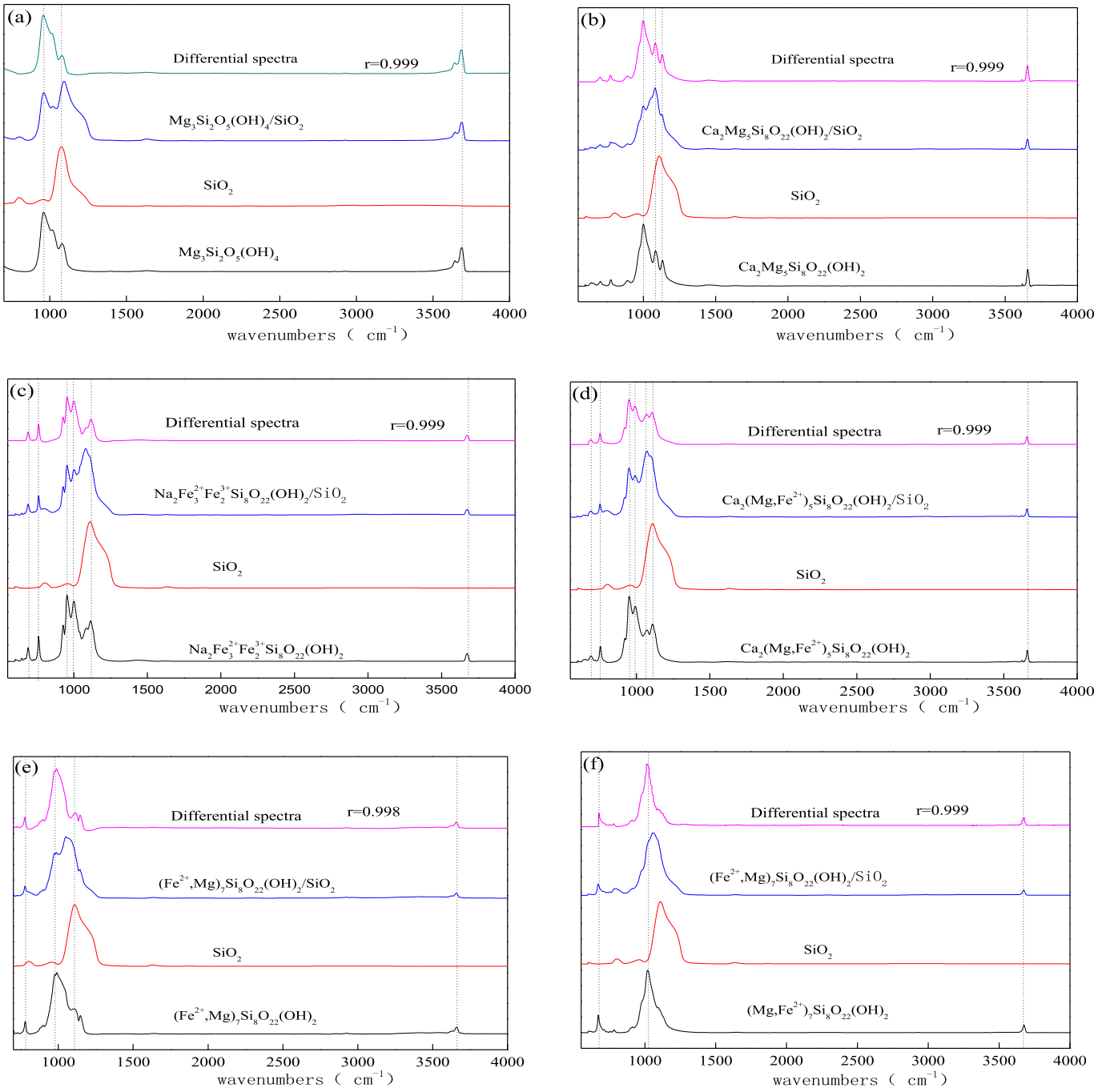

Fig. 2. Results of qualitative analyses using the differential spectrum method of mixtures of asbestos and SiO_2 particles: (a) chrysotile, (b) tremolite, (c) crocidolite, (d) actinolite, (e) amosite, and (f) anthophyllite.

comparing the sample spectra with the standard asbestos spectra, and the results are shown in Fig. 2. The spectral similarities were up to 0.999, indicating that the differential spectrum technique effectively distinguished asbestos from the other mixture components and removed interferences caused by impurities. In the quantitative analysis method, the Si concentration determined by ICP-OES was the total value for asbestos and other particles.

Quantitative analysis by FT-IR has been widely used in the medicine, food, textile, and agriculture fields [23,24]. The method is based on the Beer–Lambert law, which reflects the relationship between absorbance and concentration. Absorbance is usually represented by the height or area of a peak. The relative standard deviation of the 3686 cm^{-1} peak area for asbestos at five random points on a sample was about 0.01% (Table S2 in SI), indicating that the method was suitable for quantitatively analyzing asbestos fragments. Interference caused by particles in asbestos and particulate matter mixtures was removed using the differential spectrum method described above. This process did not change the location of the asbestos OH peak, and the relationship between the target peak area and the asbestos content was linear (Fig. S4 in SI).

Experiments were performed using simulated and environmental water samples to validate this quantitative relationship. The simulated sample was 2 mg asbestos and 2 mg SiO_2 in 1 L ultrapure water. The environmental water samples were 1 L water samples

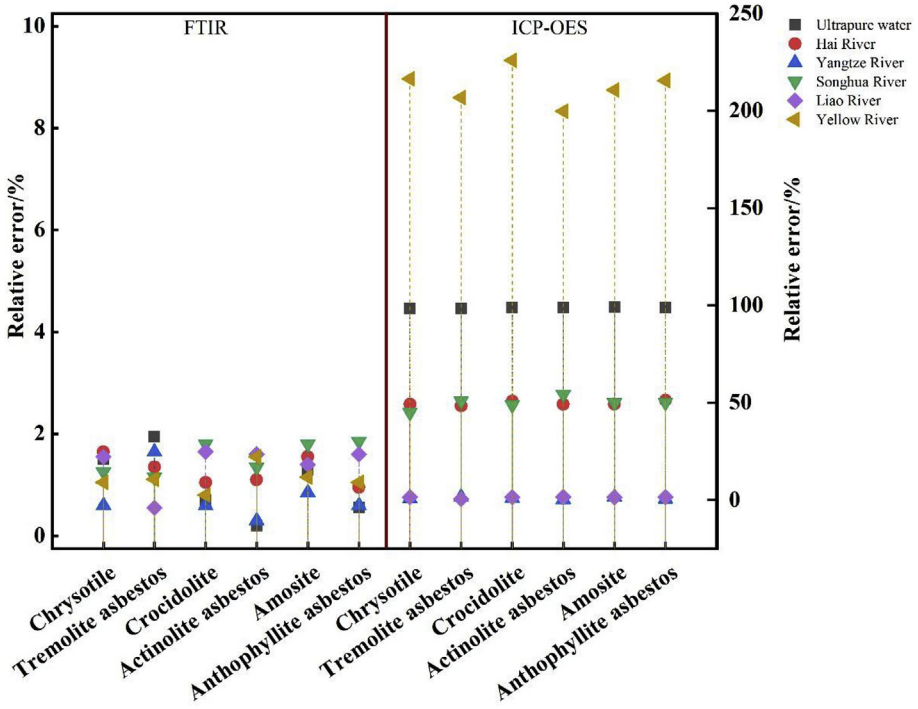

Fig. 3. The relative errors for the different river samples by FT-IR/ICP.

from the Hai River, Songhua River, Liao River, Yangtze River, and Yellow River, with 2 mg asbestos added to each sample. The quantitative results are shown in Table S3 (in SI). The relative errors and relative standard deviations were <2% and <0.1% respectively. The relative error of the ICP-OES measurements (the difference between the measured and the standard values) was <1%. The FT-IR results and ICP-OES results for the simulated water samples were similar. The asbestos concentrations measured by ICP-OES and FT-IR were different for the Yellow River, Hai River, and Songhua River samples, the concentrations determined by ICP-OES being higher than the concentrations determined by FT-IR. This could have been caused by the presence of silicate particles in the river water increasing the Si contents. For example, the presence of silicate particles caused the relative errors for the Yellow River sample to be 200%–215% using ICP-OES, but the relative errors were <2% using FT-IR (Fig. 3).

These results indicated that, if only one type of asbestos is present and sand (or kaolin) is also present, FT-IT spectra can be used to exclude interferences caused by the presence of sediment, select a non-overlapping characteristic asbestos peak, and accurately quantify the asbestos according to the Langmuir law. The Si concentration determined by ICP-OES was the total concentration of Si in asbestos and other particles.

3.4. Coupling stepwise multiple differential spectrum analysis with partial least squares analysis to quantitatively analyze multiple types of asbestos in mixtures

As mentioned in Section 3.1, a single type of asbestos mixed with silicate particles could be quantified by FT-IR using the differential

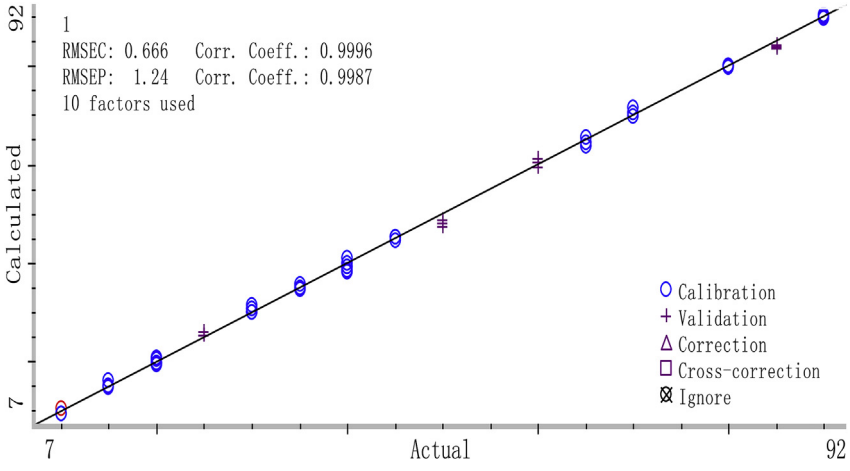

Fig. 4. Partial least squares quantitative analysis model for chrysotile and actinolite.

Table 5
Parameters for the partial least squares method for the determination of six types of asbestos in mixtures with different mass ratios.

Parameters	Chrysotile/Actinolite/Amosite/Crocidolite/Anthophyllite asbestos/Tremolite asbestos mass ratio (%)				
	5/5/5/5/40/40	10/10/10/10/30/30	15/15/15/15/20/20	20/20/20/20/10/10	30/30/25/5/5/5
Chrysotile	4.95	9.91	14.97	19.80	29.86
Relative error %	1.00	0.90	0.20	1.00	0.47
Relative standard deviation %	0.71	0.98	0.76	0.69	0.98
Actinolite	5.06	9.97	14.92	19.89	29.89
Relative error %	1.20	0.30	0.53	0.55	0.97
Relative standard deviation %	1.01	0.64	0.85	0.85	0.89
Amosite	4.96	9.92	14.90	19.93	24.91
Relative error %	0.80	0.80	0.67	0.35	0.36
Relative standard deviation %	0.98	0.76	0.71	0.77	0.81
Crocidolite	5.03	9.95	14.91	19.79	4.95
Relative error %	0.60	0.50	0.60	1.05	1.00
Relative standard deviation %	0.58	0.89	0.95	0.65	0.96
Anthophyllite asbestos	39.90	29.95	19.87	9.90	4.96
Relative error %	0.25	0.17	0.65	1.00	0.80
Relative standard deviation %	0.76	0.75	0.85	0.58	0.85
Tremolite asbestos	40.17	29.87	19.89	9.92	4.95
Relative error %	0.43	0.43	0.55	0.80	1.00
Relative standard deviation %	0.85	0.91	0.92	0.96	0.79

Table 6
Parameters for the quantitative analysis of six types of asbestos in real water by FT-IR/ICP-OES.

	Hai River	Songhua River	Liao River	Yangtze River	Yellow River
Chrysotile	**2.01**	**1.96**	**1.96**	**2.03**	**1.95**
Relative error %	0.50	2.00	2.00	1.50	2.50
Relative standard deviation %	0.78	1.09	0.77	0.52	0.3
Actinolite asbestos	**3.98**	**4.05**	**4.01**	**3.95**	**4.02**
Relative error %	0.50	1.25	0.25	1.25	0.50
Relative standard deviation %	0.63	0.25	0.9	0.67	0.69
Amosite	**6.02**	**5.97**	**6.05**	**5.98**	**6.06**
Relative error %	0.33	0.17	0.83	0.36	1.00
Relative standard deviation %	0.58	0.26	0.25	0.6	0.69
Crocidolite	**1.98**	**2.04**	**1.97**	**1.96**	**2.02**
Relative error %	1.00	2.00	1.50	2.00	1.00
Relative standard deviation %	0.81	0.83	0.78	0.90	0.98
Anthophyllite asbestos	**4.02**	**4.05**	**3.97**	**3.90**	**3.95**
Relative error %	0.50	1.25	0.75	2.50	1.25
Relative standard deviation %	0.90	0.82	0.91	0.96	0.81
Tremolite asbestos	**5.96**	**6.03**	**6.01**	**5.98**	**6.04**
Relative error %	0.67	0.50	0.17	0.33	0.67
Relative standard deviation %	0.81	0.79	0.86	0.96	0.91

spectrum method. This was not possible for multiple types of asbestos because the characteristic FT-IR peaks for different types of asbestos were close together or even overlapped. It need to use the partial least squares method. We used chrysotile and actinolite as examples, and attempted to validate and calibrate the method by coupling the stepwise multiple differential spectrum method with partial least squares analysis to quantitatively analyze multiple types of asbestos in a mixture. The characteristic FT-IR peaks for chrysotile and actinolite were at almost the same wavenumber (Fig. S5 in SI). The partial least squares method was therefore used to quantify the different types of asbestos. Chrysotile and actinolite were added to samples of ultrapure water at specified ratios, the samples were subjected to the pretreatment method described in Section 2.2.4, then the FT-IR spectra of the mixtures were acquired. The chrysotile and actinolite concentrations were determined by differentiating the FT-IR spectra, and the similarities between the

Fig. 5. Photograph of asbestos fibers in mouse liver.

differential spectra and the spectra of standards of the two types of asbestos were determined. As shown in Fig. S6 (in SI), the similarities were up to 0.999, indicating that the differential spectrum partial least squares method is an effective way of determining the asbestos content of a mixture.

The partial least squares method in TQ Analyst software (Thermo Fisher) was used to perform the quantitative analysis. The FT-IR peak range was 620–3676 cm^{-1}, and 25 and 75 portions of the FT-IR spectra were used in the validation and calibration processes, respectively. The chrysotile and actinolite calibration curves are shown in Fig. 4.

In Fig. 4, R, RMSEC, and RMSEP are the regression coefficient, root mean square error, and root mean square prediction error, respectively. The R, RMSEC, and RMSEP values were 0.9996, 0.666, and 1.24, respectively, indicating that the method was very stable and had a good prediction ability.

A library of FT-IR spectra of chrysotile and actinolite was obtained, and the mass ratio was determined by coupling the stepwise multiple differential spectrum method with the partial least squares method. The chrysotile or actinolite content was calculated from the total asbestos content determined by ICP-OES.

The stepwise multiple differential spectrum method was then

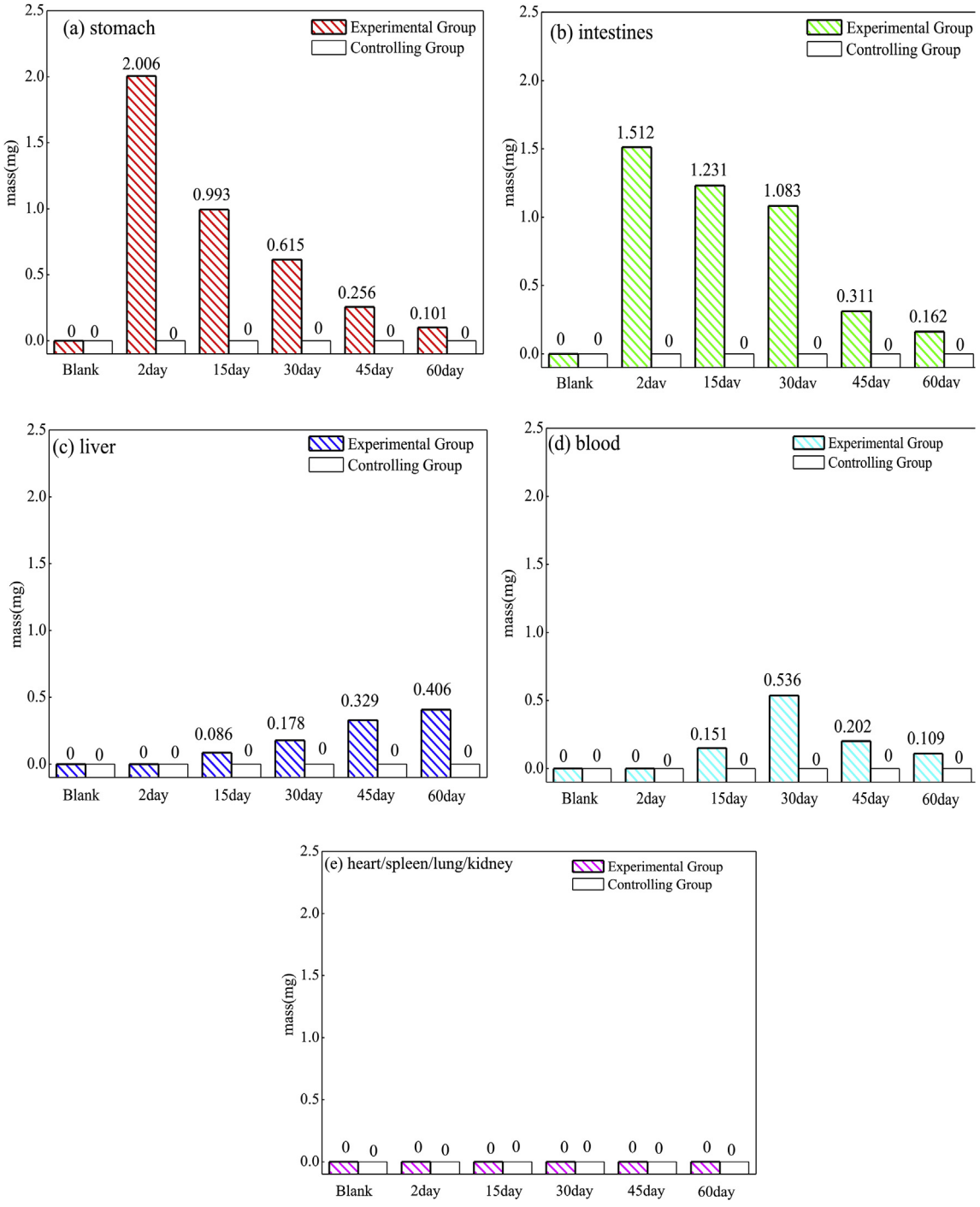

Fig. 6. Asbestos contents in mouse (a) stomach, (b) intestine, (c) liver, (d) blood, and (e) heart/spleen/lung/kidney at different times after asbestos ingestion stopped.

used to obtain the FT-IR spectrum of each type of asbestos. The six types of asbestos were numbered 1–6 (1 chrysotile, 2 tremolite, 3 crocidolite, 4 actinolite, 5 amosite, and 6 anthophyllite). Mixed asbestos samples were pretreated, then the FT-IR spectrum of each type of asbestos was acquired by applying the stepwise multiple differential FT-IR spectrum method on the mixed sample spectra (see Fig. S7 in SI). The similarities for the FT-IR spectra were ~0.999. The partial least squares method was then used to determine the asbestos content. The six types of asbestosas mentioned before were added to ultrapure water at specified mass ratios. The FT-IR spectra of the suspensions were determined using the partial least squares method, and the results are shown in Table 5. The relative errors and relative standard deviations were <5%, <3% respectively.

Interferences caused by other materials (e.g., silicates and natural organic materials) should be taken into account when determining asbestos. This was addressed by adding 2 mg chrysotile, 4 mg actinolite, 6 mg amosite, 2 mg crocidolite, 4 mg anthophyllite, and 6 tremolite to 1 L water samples from the Hai River, Songhua River, Liao River, Yangtze River, and Yellow River. The samples were pretreated and then quantitatively analyzed. The relative errors and relative standard deviations were <2%, <1% respectively (Table 6). These results indicated that coupling the stepwise multiple differential spectrum method and partial least squares method effectively allowed different types of asbestos to be quantitatively analyzed.

3.5. Asbestos transport through the organs and blood of mice

Asbestos used in pipes in drinking water systems can be transferred to the water being transported. It is important to note that insufficient evidence has been acquired for a toxic mechanism indicating asbestos in drinking water poses risks to humans and animals. No consistent conclusions can therefore be drawn about the risks posed by asbestos in drinking water, and this has hindered the development of criteria for controlling asbestos in drinking water following World Health Organization water quality standards. The method described above could be used to qualitatively and quantitatively determine asbestos in water to provide evidence to improve this situation.

White asbestos fibers can clearly be seen in the mouse liver image shown in Fig. 5, acquired using an OLYMPUS BX51 system with a magnification of 40 (Olympus, Tokyo Japan). This is direct evidence for asbestos accumulating in the liver. We assumed that the asbestos was transferred to the liver after being ingested and absorbed.

The FT-IR and ICP-OES methods were used to improve our understanding of the migration of ingested asbestos in animals. The changes in the asbestos concentrations in the mouse stomachs, intestines, blood, livers, hearts, spleens, lungs, and kidneys over time are shown in Fig. 6. The No. 1 mice were fed 5 mg asbestos for 5 d, then drinking water and nutrient solution (instead of the chrysotile suspension). On the second day after feeding asbestos stopped 3.5 mg of asbestos remained in the mice, and the asbestos was mainly in the stomach (2.006 mg) and intestines (1.512 mg). As time increased, the asbestos contents of the stomach and intestines decreased from 2.006 to 0.101 mg and from 1.512 to 0.162 mg, respectively, but the asbestos content of the blood had increased to 0.536 mg on the 30th day but then decreased to 0.109 mg on the 60th day. Interestingly, the asbestos content of the liver kept increasing, from 0 to 0.406 mg, throughout the study. Asbestos was not found in the heart, spleen, lung, or kidney (Fig. 6e). The total amounts of asbestos in the mice decreased over time. These results indicate that ingested asbestos enters the digestive system (stomach and intestines) and becomes absorbed into the gastrointestinal mucosa. Some of the asbestos can then enter the blood and may accumulate in the liver or be excreted.

4. Conclusions

This study was focused on the quantitative analysis of asbestos in mixtures, particularly asbestos in groundwater and drinking water, by FT-IR. A method for quantitatively analyzing asbestos in mixtures by FT-IR and ICP-OES was developed. The detection limit of six kinds of asbestos by using ICP-OES and FT-IR in water are respectively from 0.0139 to 0.0209 mg/L, from 0.0012 to 0.0019 mg/L, and the quantification limit of six kinds of asbestos by using inductively coupled plasma optical emission spectrometry and Fourier-transform infrared spectroscopy in water are respectively from 0.0468 to 0.0705 mg/L, from 0.0039 to 0.0064 mg/L. The relative standard deviations were respectively less than 2.85% and 3.81%. The relative recovery was calculated by percentage of the analytes recovered. The recoveries of the test asbestos were respectively more than 95.10% and 95.38%. The results indicated that asbestos in a mixture (e.g., with silicates and sand) could be quantitatively analyzed using the differential spectrum method, stepwise multiple differential spectrum method, and partial least square method. The migration of ingested asbestos in mice was investigated, and it was found that little asbestos remained in the stomach, intestine, and blood after 60 d but that a large amount remained in the liver. We concluded that asbestos fibers in water could cause unpredictable risks to humans. Further studies using the analytical technique proposed here are urgently required.

Declaration of interest statement/conflict of interest

The authors declare that we have no financial and personal relationships with other people or organizations that can inappropriately influence our work, there is no professional or other personal interest of any nature or kind in any product, service and/or company that could be construed as influencing the position presented in, or the review of, the manuscript entitled, “Quantitative analysis of asbestos in drinking water and its migration in mice using Fourier-transform infrared spectroscopy and inductively coupled plasma optical emission spectrometry”.

Acknowledgements

This work was supported by the Major Science and Technology Program for Water Pollution Control and Treatment, China [grant number 2014ZX07402001]. We thank Gareth Thomas, PhD, from Liwen Bianji, Edanz Group China (www.liwenbianji.cn/ac), for editing the English text of a draft of this manuscript. The authors gratefully acknowledge the contributions of Prof. Shifu Weng (College of Chemistry and Molecular Engineering, Peking University).

Appendix A. Supplementary data

Supplementary data to this article can be found online at https://doi.org/10.1016/j.aca.2018.12.022.

References

[1] M.S. Kanarek, P.M. Conforti, L.A. Jackson, Chrysotile asbestos fibers in drinking water from asbestos-cement pipe, Environ. Sci. Technol. 15 (1981) 923–925.
[2] D. Wang, R. Culluinore, Y. Hu, Biodeterioration of asbestos cement(AC)pipe in drinking water distribution system, Int. Biodeterioration Biodegradation 65 (2011) 810–870.
[3] X.T. Chen, N.W. Tao, D.F. Zeng, S.W. Jiang, Introduction of test methods for asbestos in ship materials, Dev. Appl. Mater. 1 (2014) 79–88.

[4] B. Fubini, I. Fenoglio, Toxic potential of mineral dusts, Elements 3 (2007) 407–414.
[5] B.T. Mossman, M. Lippmann, T.W. Hesterberg, K.T. Kelsey, A. Barchowsky, J.C. Bonner, Pulmonary endpoints (lung carcinomas and asbestosis) following inhalation exposure to asbestos, J. Toxicol. Environ. Health B 14 (2011) 76–121.
[6] V.C. Sanchez, J.R. Pietruska, N.R. Miselis, R.H. Hurt, A.B. Kane, Biopersistence and potential adverse health impacts of fibrous nanomaterials: what have we learned from asbestos? Wiley Interdiscip. Rev. Nanomed.Nanobiotechnol 1 (2009) 511–529.
[7] D. Bernstein, V. Castranova, K. Donaldson, B. Fubini, J. Hadley, T. Hesterberg, A. Kane, D. Lai, E.E. McConnell, H. Muhle, G. Oberdorster, S. Olin, D.B. Warheit, Testing of fibrous particles: short-term assays and strategies: report of an ILSI Risk Science Institute Working Group, Inhal. Toxicol. 17 (2005) 497–537.
[8] K. Unfried, C. Schurkes, J. Abel, Distinct spectrum of mutations induced by crocidolite asbestos clue for 8-hydroxydeoxyguanosine-dependent mutagenesis in vivo, Cancer Res. 62 (2002) 99–104.
[9] A. Bloise, D. Barca, A.F. Gualtieri, S. Pollastri, E. Belluso, Trace elements in hazardous mineral fibres, Environ. Pollut. 216 (2016) 314–323.
[10] G.R. Gulino, M. Polimeni, M. Prato, E. Gazzano, J. Kopecka, S. Colombatto, D. Ghigo, E. Aldieri, Effects of chrysotile exposure in human bronchial epithelial cells: insights into the pathogenic mechanisms of asbestos-related diseases, Environ. Health Perspect. 124 (2016) 776–785.
[11] D.W. Kamp, Asbestos-induced lung diseases: an update, Transl. Res. 153 (2009) 143–152.
[12] H.E. Ayer, J.R. Lynch, J.H. Fanney, A comparison of impinger and membrane filter techniques for evaluating air samples in asbestos plants, Ann. N. Y. Acad. Sci. 132 (1965) 274–287.
[13] T. Schneider, The influence of counting rules on the number and on the size distribution of fibres, Ann. Occup. Hyg. 21 (4) (1978) 341–350.
[14] K.R. Senthil, P. Rajkumar, Characterization of minerals in air dust particles in the state of Tamilnadu, India through FT-IR spectroscopy, Atmos. Chem. Phys. Discuss. 273 (5665) (2013) 22221–22248.
[15] F. Liu, Y.H. Jiang, Y. He, Variable selection in visible/near infrared spectra for linear and nonlinear calibrations: a case study to determine soluble solids content of beer, Anal. Chim. Acta 635 (1) (2009) 45–52.
[16] F. Liu, Y.H. Jiang, Y. He, Variable selection in visible/near infrared spectra for linear and nonlinear calibrations: a case study to determine soluble solids content of beer, Anal. Chim. Acta 635 (1) (2009) 45–52.
[17] F.C.S. Sófacles, K.H.G. Roberto, C.U.A. Mário, C.S. Edvan, F.P. Claudete, I.E.A. Stéfani, C. Flaviano, A modification of the successive projections algorithm for spectral variable selection in the presence of unknown interferents, Anlytica Chimica Acta 689 (1) (2011) 22–28.
[18] Li Yang, Qinghua Yan, Yinping Cao, Huirong Zhang, Determination of mineral elements of some coarse grains by microwave digestion with inductively coupled plasma atomic emission spectrometry, J. Chem. 9 (1) (2012) 93–98.
[19] Y.F. Lu, H.E. Allen, A predictive model for copper partitioning tosuspended particulate matter in river waters, Environ. Pollut. 143 (1) (2006) 60–72.
[20] G.F. Graun, Waterborne outbreaks of cryptosporidiosis, J. Am. Water Works Assoc. 90 (9) (1998) 81–91.
[21] D. Leland, A cryptosporidiosis break in a filtered water supply, J. Am. Water Works Assoc. 85 (6) (1992) 34–42.
[22] H. Tom, C. Brian, Particle counters as tools for managing cryptosporidium risk in water treatment, Water Sci. Technol. 36 (4) (1997) 143–149.
[23] Z.B. Su, S.Y. Jiang, IR featlires of the minerals assoclated with chrysotile asbestos, J. Mineral. Petrol. 3 (1984) 102–108.
[24] N. Abidi, L.C.E. Hequet, Fourier transform infrared spectroscopic approach to the study of the secondary cell wall development in cotton fiber, Cellulose 17 (2) (2010) 309–320.